

Figure S1 Printing of the navigational template. The model of the whole template is shown from the front view (A1) and back view (A2). The navigational template was further divided into three parts: landmark recognition part, needle insertion part, and connecting part, which are shown in blue, red, and light yellow, respectively (B). Two parts recognizing the sternal end of the clavicle and the costal arch were included in the novel design, and are shown in purple and orange (C). After the completion of the design, the whole navigational template was printed using stereolithography from photopolymer material (D).

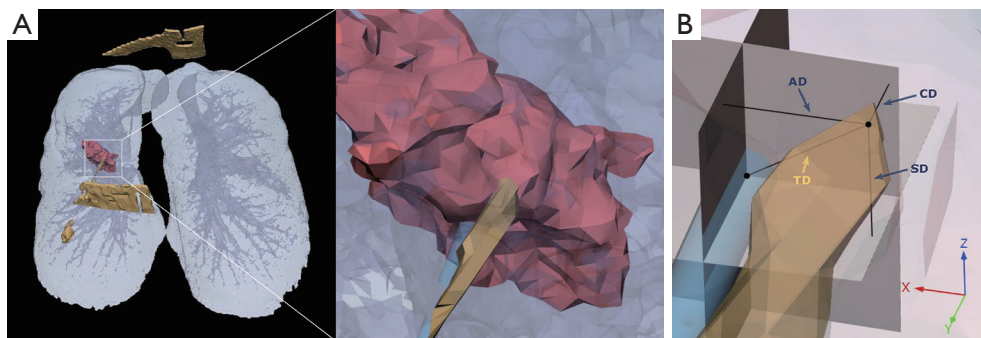


Figure S2 Deviation calculation method. The digital model of the lung (purple part), the lesion (red part), the designed insertion route (blue cylinder), and the real position of the template and biopsy needle (yellow part) was reconstructed (A). A rectangular coordinate system was established with the origin of the end of the designed route. AD, CD, and SD were measured separately, and TD was then calculated (B). AD, axial deviation; CD, coronal deviation; SD, sagittal deviation; TD, total deviation.

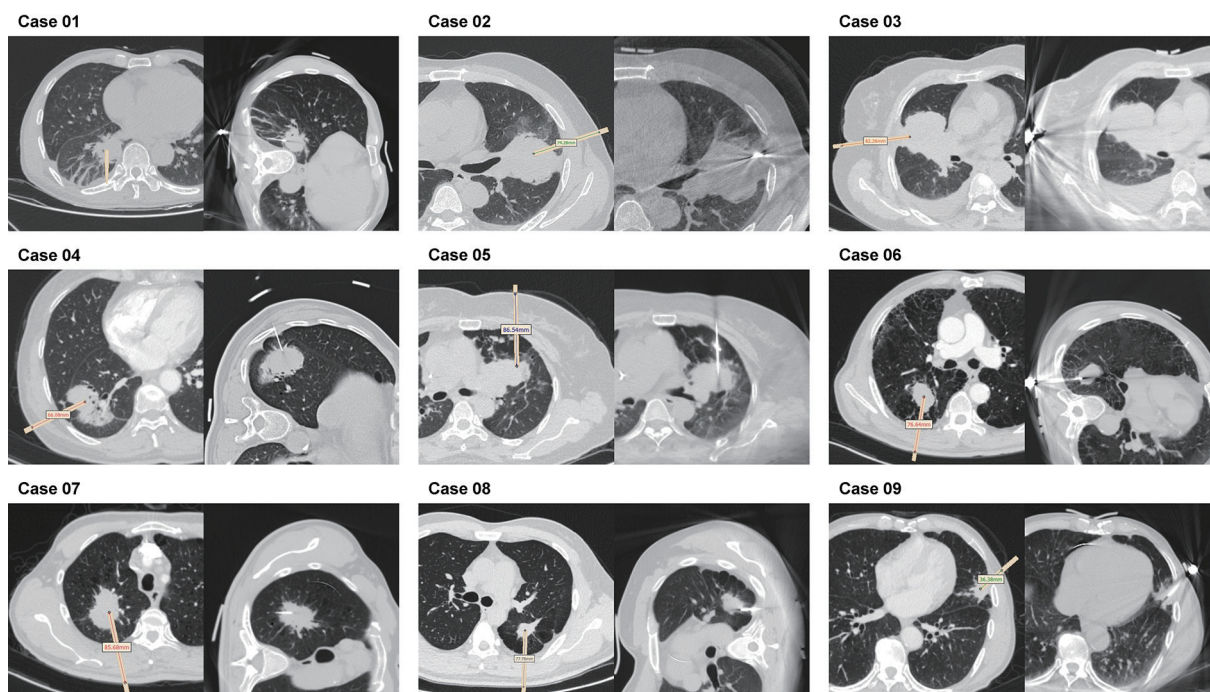


Figure S3 CT images of the 17 successful cases (Figures S3,S4). All the successful cases are presented according to the recruitment order. The CT images of insertion route design and real needle insertion were compared in every case. Cases 1 to 9 are included in this figure. CT, computed tomography.

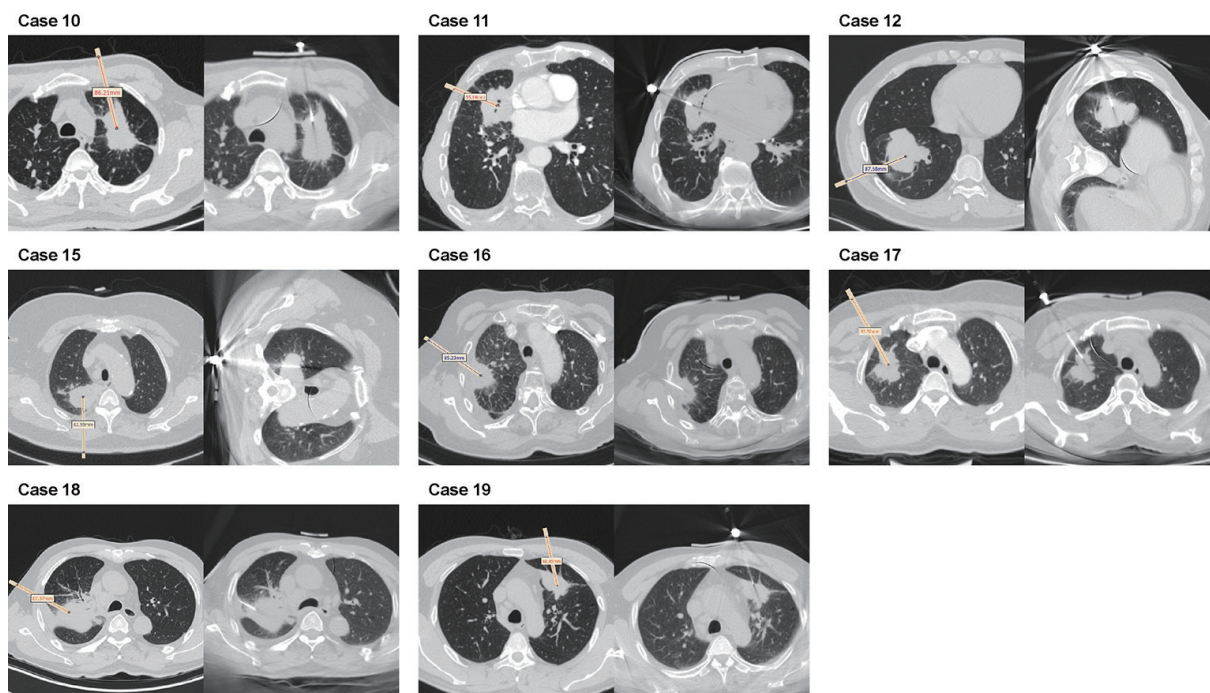


Figure S4 CT images of the 17 successful cases (Figures S3,S4). The CT images of insertion route design and real needle insertion of the other 8 successful cases are presented. Cases 13 and 20 were 2 patients who dropped out during the study, and case 14 was the case of template-guided biopsy failure. Hence, the CT images of these 3 cases are not shown in the figure. CT, computed tomography.

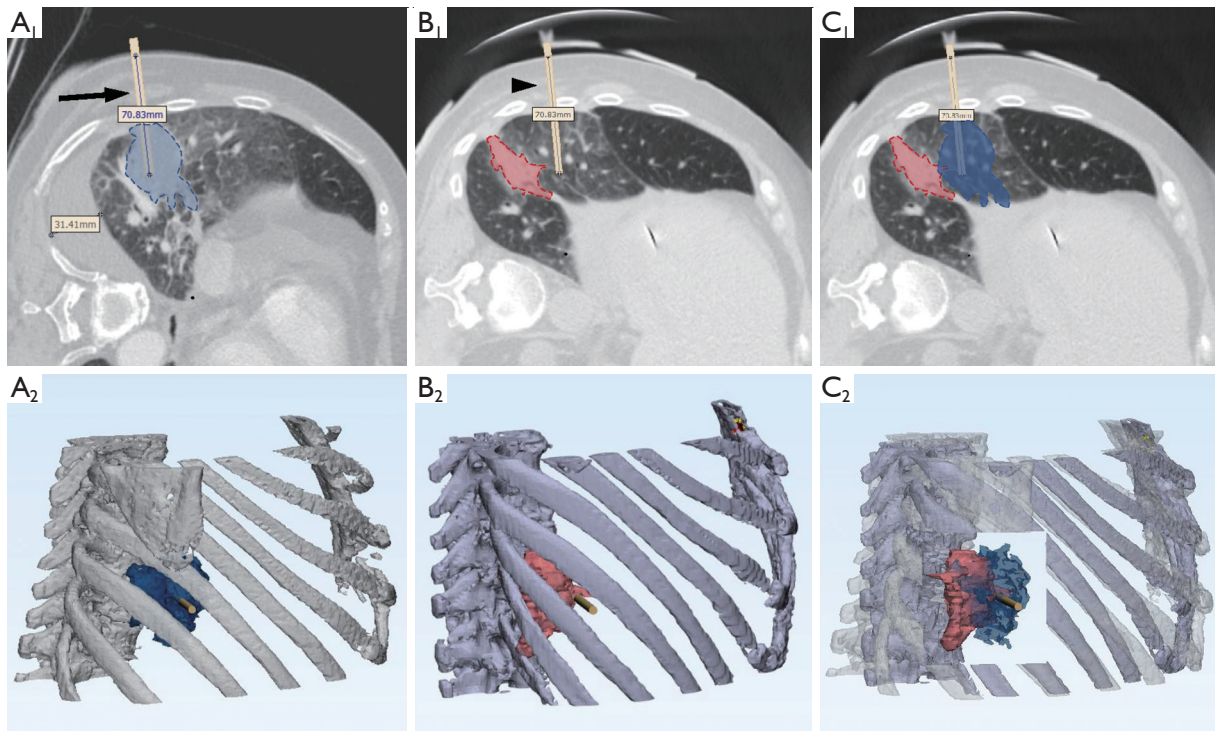


Figure S5 A failed case of template-guided FNA. The pre-biopsy CT image revealed a pleural effusion which measured 31.4 mm in the long-axis diameter in the right thoracic cavity (A1, the CT image is rotated 90° clockwise, and the blue part represents the target lesion). The designed insertion route (pointed by a black arrow) was through the right eighth intercostal space (A2, the route is indicated by a cylinder). When the participant adopted the lateral decubitus position for biopsy, the relative position between the thoracic cage and the lesion (red part) altered (B1,B2). The lesion could not be targeted through the predesigned route (pointed by a black arrowhead). The alteration of the lesion's position is clearly shown in the CT image and the reconstructed model (C1,C2). FNA, fine-needle aspiration; CT, computed tomography.

Table S1 Specific clinical characteristics of the 17 successful cases

Enrollment number	Sex	Age, years	BMI, kg/m ²	Nodule size, mm	Distance between lesion and pleura, mm	Nodule location	Biopsy type	Decubitus position	Length of the insertion route, mm
1	Male	66	20.20	39.3	11.2	RLL	FNA + CNB	Lateral	78.1
2	Male	61	25.71	56.0	0.0	LUL	FNA	Supine	74.3
3	Female	67	23.73	66.3	0.0	RML	FNA + CNB	Supine	82.3
4	Female	62	20.23	52.6	5.3	RLL	FNA	Lateral	66.1
5	Female	58	24.67	45.5	9.4	LUL	FNA + CNB	Supine	86.5
6	Male	70	22.76	38.3	16.6	RUL	FNA + CNB	Lateral	76.6
7	Male	64	19.59	45.5	4.4	RUL	FNA	Lateral	85.7
8	Male	37	25.91	32.4	5.3	LUL	FNA + CNB	Lateral	77.8
9	Male	72	21.08	31.7	0.0	LUL	FNA + CNB	Supine	36.4
10	Male	52	23.18	51.7	0.0	LUL	FNA	Supine	86.2
11	Male	74	17.81	41.4	15.9	RML	FNA	Supine	55.2
12	Male	45	27.73	52.5	11.4	RLL	FNA + CNB	Lateral	87.7
15	Female	65	29.69	41.0	0.0	RUL	FNA	Lateral	82.6
16	Female	75	24.98	33.4	0.0	RUL	FNA	Supine	85.2
17	Female	44	23.92	36.6	0.0	RUL	FNA	Supine	83.5
18	Male	59	20.96	44.2	0.0	RUL	FNA	Supine	87.6
19	Male	46	25.95	34.8	13.9	LUL	FNA	Supine	69.0

BMI, body mass index; RLL, right lower lobe; LUL, left upper lobe; RML, right middle lobe; RUL, right upper lobe; FNA, fine-needle aspiration; CNB, core needle biopsy.

Table S2 Specific clinicopathological information of the 17 successful cases

Enrollment number	Insertion deviation, mm				Procedural duration, min	DLP, mGy×cm	Complication	Cytological examination result
	CD	AD	SD	TD				
1	13.02	7.69	1.26	15.17	11.8	223.5	PNX	Adenocarcinoma
2	6.67	0.28	1.12	6.77	10.6	218.7	None	Poorly differentiated
3	0.86	5.42	3.12	6.31	10.8	249.3	None	Adenocarcinoma
4	1.07	7.24	5.94	9.43	11.9	187.1	None	Adenocarcinoma
5	1.34	6.71	0.52	6.86	10.7	179.6	None	Non-small cell carcinoma
6	0.11	10.65	0.35	10.66	9.7	173.0	None	Poorly differentiated
7	6.39	3.86	9.24	11.88	11.8	195.6	None	Non-small cell carcinoma
8	5.28	4.44	12.45	14.23	10.4	249.6	None	Inadequate sample
9	0.44	0.60	7.77	7.81	7.8	232.0	Pulm. Hem.	Suspicious for malignancy
10	2.10	2.48	4.25	5.35	11.3	201.5	Pulm. Hem.	Non-small cell carcinoma
11	1.53	2.29	9.45	9.84	9.7	256.0	None	Inadequate sample
12	3.72	2.43	11.88	12.68	7.1	207.1	PNX	Non-small cell carcinoma
15	6.30	8.00	1.50	10.29	13.3	231.0	None	Inadequate sample
16	0.63	9.21	6.78	11.45	6.4	220.9	None	Adenocarcinoma
17	0.53	7.35	2.61	7.82	9.7	211.4	None	Adenocarcinoma
18	3.05	1.51	3.20	4.67	11.6	253.4	Pulm. Hem.	Adenocarcinoma
19	4.75	0.06	5.92	7.59	13.5	288.6	None	Non-small cell carcinoma

CD, coronal deviation; AD, axial deviation; SD, sagittal deviation; TD, total deviation; DLP, dose-length product; PNX, pneumothorax; Pulm. Hem., pulmonary hemorrhage.

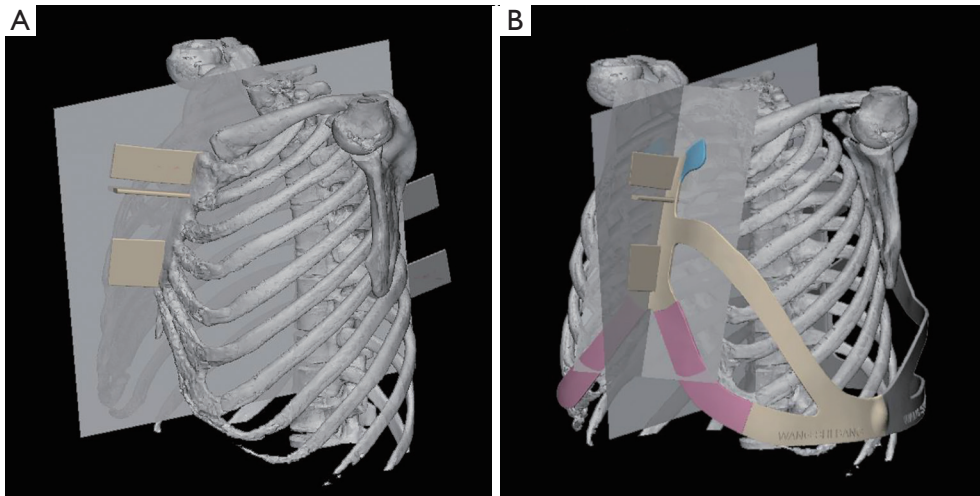


Figure S6 Indications of the newly-selected landmarks. The routinely chosen skeletal landmarks lay approximately in the same sagittal plane (A). Additional parts recognizing the sternal end of the clavicle (blue part) and the costal arch (red part) were added to the design of the template for reconfirming the position in the coronal plane (B).